



Synthesis of smooth amorphous thin films of silicon carbide with controlled properties through pulsed laser deposition

Mohamed Oujja¹ · Karima Tabakkouht¹ · Mikel Sanz^{1,2} · Esther Rebollar¹ · María Sánchez-Arenillas¹ · José F. Marco¹ · Marta Castillejo¹ · Rebeca de Nalda¹

Received: 9 December 2021 / Accepted: 17 March 2022 / Published online: 5 April 2022
© The Author(s) 2022

Abstract

Thin films of silicon carbide (SiC) on Si (100) and SrTiO₃ (100) substrates have been grown by nanosecond pulsed laser deposition (PLD) with a *Q*-switched Nd:YAG laser operating at the wavelengths of 1064, 532 and 266 nm. The deposits obtained consisted of smooth and uniform layers of amorphous SiC, free of holes and cracks, with thicknesses in the range of 30–100 nm and average roughness substantially lower than 1 nm. The role of laser wavelength and of substrate temperature (300 K vs. 1025 K) on morphology, crystallinity and composition of the deposits was assessed. The films were analyzed by X-ray diffraction, micro-Raman spectroscopy and X-ray photoelectron spectroscopy. In addition, optical emission spectroscopy was employed to evaluate the characteristics of the ablation plasma and its correlation with the film growth.

Keywords Pulsed laser deposition · Thin films · Silicon carbide · Multianalytical approach

1 Introduction

Silicon carbide (SiC) is an indirect wide bandgap semiconductor with adequate electronic characteristics for high-power, high-frequency and high-temperature electronic devices [1]. Moreover, SiC is a superhard ceramic with superior mechanical and thermal properties such as very high hardness (9 on Moh's scale), high melting point, chemical and thermal stability, oxidation resistance and low density, making it appropriate for the fabrication of abrasion tools and cutting applications [2]. With respect to biological applications, SiC is biocompatible, and as such it can be applied as coating on biomedical implants or as a semipermeable biomaterial [3]. In nanostructured form, SiC is suitable for applications to photonics, energy storage and conversion, microelectronics, nanoelectronics and life sciences [4].

In its amorphous phase (a-SiC), silicon carbide shows appealing physical properties such as hardness and high Young's modulus, high optical transmission in the visible region of the spectrum and variable optical gap [5–7]. In addition, a-SiC is a suitable material to improve the tribological behavior of surfaces or to enhance device reliability and lifetime [8]. However, those same favorable properties make SiC a difficult material to process and control. Therefore, it is critical to optimize the properties and control the microstructure of the deposited a-SiC films, either by developing new processing routes or by determining optimum windows of operating conditions.

From the beginning of the 80s, chemical vapor deposition (CVD) has become the most common method for SiC thin film synthesis [9]. The CVD-based techniques, such as metal organic chemical vapor deposition (MOCVD) [10], hot-wire chemical vapor deposition (HW-CVD) [7, 11], plasma enhanced chemical vapor deposition (PECVD) [12] and hot filament chemical vapor deposition (HFCVD) [13], produce crystalline SiC thin films at high temperature or amorphous SiC at moderate temperature.

Pulsed laser deposition (PLD) offers several advantages for thin film synthesis over other techniques: simple experimental setup with flexibility and broad range of controllable deposition parameters, such as temperature, pressure, wavelength or laser fluence [14, 15]. Unlike other deposition

✉ Mohamed Oujja
m.oujja@iqfr.csic.es

✉ Rebeca de Nalda
r.nalda@iqfr.csic.es

¹ Instituto de Química Física Rocasolano, CSIC, Serrano 119, 28006 Madrid, Spain

² Present Address: Facultad de Ciencias, Universidad Nacional de Educación a Distancia (UNED), Senda del Rey 9, 28040 Madrid, Spain

methods, neutral and ionized species with considerable kinetic energy (in the range from 1 to 100 eV) are ejected by laser ablation. Upon impact with the substrate, they can raise the local temperature while keeping the rest of the substrate at a lower temperature [16]. Over the last years, PLD has proven to be an alternative synthesis technique that allows deposition of hydrogen-free amorphous and crystalline SiC films on various substrates [17]. Many previous PLD studies have targeted the growth of polycrystalline SiC films; it is generally accepted that this requires substrate temperatures above 1075 K. However, these temperatures are not universally withstood by all substrate materials, and problems linked to the high thermal expansion coefficient and Young's modulus of polycrystalline SiC can lead to cracking in protective coating applications. Therefore, the growth of high-quality amorphous SiC films is desirable.

The properties of PLD-grown SiC can be controlled by changing the deposition parameters, as has been shown in some previous studies [5, 6, 18–26]. In particular, the effect of deposition temperature, post-deposition annealing and laser energy on the nanostructure, bonding and crystalline properties of the films has been studied. Most PLD investigations of SiC thin films have been performed with UV lasers, generally in an attempt to minimize the presence of particulates on the resulting films, therefore disregarding the use of IR irradiation for the production of quality SiC films [17]. Nevertheless, some of the few exceptions have shown that the use of IR PLD can produce well adherent, particulate free thin films of 3C-SiC [27].

The study of amorphous SiC grown by PLD at different substrate temperatures has shown that an important transition exists in the region of 875 K. Across this transition, the nanostructure of the films suffers a dramatic change linked with reduced disorder, more uniform environment of the Si–C bonds and higher density [5, 6, 18, 21]. In addition, it has been reported [5] that the mechanical properties of a-SiC films are fundamentally determined by the density of Si–C bonds, with both the hardness and the elastic modulus showing a constant plus linear dependence on the number of Si–C bonds across a large range. In this sense, it is important to optimize the conditions for the growth of amorphous SiC films with the highest possible bond density.

This work describes a study where the role of laser wavelength has been combined with substrate temperature (T_s) to explore the possibilities for the control of the growth of silicon carbide thin films by PLD. We report on the fabrication of thin films of SiC on Si (100) and SrTiO₃ (100) substrates heated to different temperatures (300 K and 1025 K) by nanosecond PLD of silicon carbide in vacuum from the UV to the IR (at the wavelengths of 1064, 532 and 266 nm). The deposits have been characterized in their morphology, structure and composition by atomic force microscopy (AFM), X-ray diffraction (XRD), X-ray photoelectron spectroscopy

(XPS) and micro-Raman spectroscopy. At the same time of film fabrication, the features of the ablation plasma were studied by optical emission spectroscopy (OES) to obtain further information about the film formation process in correlation with the plasma properties.

2 Experimental details

The deposition experiments were carried out in a PLD machine described elsewhere [28]. It consists of a stainless steel vacuum chamber operated at a vacuum level of 2×10^{-4} Pa where the SiC targets are placed on a rotating holder. Ablation was produced by a *Q*-switched Nd:YAG laser (full width at half-maximum 15 ns, 10 Hz, 1064 nm) working at its fundamental wavelength and at the second and fourth harmonics (532 nm and 266 nm). Laser incidence on the target was fixed at 45°, causing an elliptic irradiation area with 0.6 and 0.3 mm major and minor axes, respectively. The threshold fluences were determined by measuring the minimum single pulse energy necessary to yield a luminous plume as detected by eye and the diameter of the irradiated region, by the print left on an unplasticized polyvinyl chloride sheet. With this criterion, fluence threshold values obtained for 266, 532 and 1064 nm were 0.26, 0.8 and 0.8 J/cm², respectively. Fluences applied for PLD growth were set to a value sufficiently above the threshold.

The targets are silicon carbide discs (10 mm in diameter and 1.5 mm in thickness) obtained from a rod (10 mm in diameter and 100 mm in length) purchased commercially (Goodfellow). Square-shaped, 10 × 10 mm strontium titanate, STO (100), or silicon, Si (100) wafers were used as substrates for PLD. The STO (100) substrates, which were used to be able to perform cleaner XPS measurements of films deposited on a Si-free substrate, were used as received from the manufacturer. In turn, Si (100) substrates were ultrasonically degreased in acetone and methanol for 10 min. They were mounted on a holder that can be heated. Experiments were conducted at 300 K (room temperature) and 1025 K. Target-substrate distance was set to 4 cm. The growth time was 2 h, corresponding to 72,000 laser pulses.

During the PLD process, spontaneous emissions from the luminous plasma were monitored in the spectral range of 300–600 nm. The spectrograph used (Kymera 193i-A, 1200 lines per mm grating) was coupled to a time-gated intensified CCD camera (iStar, Andor Technologies, 1024 × 1024 pixels, 13 μm × 13 μm pixel size). The temporal width of the detection gate applied to the CCD camera was fixed at 100 ns.

The set of films obtained under the conditions described above were characterized by a range of analytical techniques. AFM examination was performed with a Bruker Multimode 8, equipped with a Nanoscope V controller,

for determination of thickness and morphology. It was operated in tapping mode with gold-coated silicon probes (Tap300GB-G). The resulting images were analyzed using the Nanoscope Analysis 1.50 software. The analysis yielded values for the average thicknesses (measured in areas at the edge of a mask) and roughness (R_a) of the deposited films.

X-ray diffraction measurements were carried out using a Philips Xpert apparatus. The source employed was Cu K_α (1.541 Å) radiation and the configuration was $\theta/2\theta$.

The Raman response of the samples was evaluated with a Thermo Fischer DXR Raman microscope (West Palm Beach, FL 33,407, USA) that examines a region of around 2 μm diameter. The source was a 5 mW laser emitting 532 nm light. Raman spectra were acquired through the $\times 10$ objective of the confocal microscope and with 4 cm^{-1} spectral resolution. Both the operation of the equipment and data analysis were performed with the OMNIC 1.0 software.

The XPS study was carried out using Al $K\alpha$ radiation at photon energy $h\nu = 1486.6\text{ eV}$. The experiments were performed in ultra-high vacuum ($< 2 \times 10^{-9}$ mbar) using a PHOIBOS-150 electron analyzer, at an electron take-off angle of 90° . The analyzer pass energy was 20 eV. The scale of the binding energy was referenced to the C 1s signal of the adventitious carbon layer (284.6 eV). Measured spectra were fitted with the CasaXPS software using pseudo Voigt line profiles and a Shirley background. The Lorentzian/Gaussian mix ratio and full width at half-maximum were fixed across the data series.

3 Results and discussion

3.1 Description of the emission plasma

As mentioned above, an in situ probe of the PLD process was employed through the spectrally selected observation of spontaneous emissions from the luminous ablation plasma. These measurements are shown in Fig. 1, which contains the emission spectra obtained upon 1064, 532 and 266 nm irradiation corresponding to light emitted from the region immediately above the surface of the SiC target. The spectral region 375–475 nm was selected because it provides the most relevant information about the plasma in the three conditions described above. The spectra are time-gated so that emission produced during the first 100 ns after ablation are acquired. For these short delays, the spectra contain a continuous emission, which is due to short-lived ($< 50\text{ ns}$) inverse Bremsstrahlung. The discrete lines can be assigned to neutral atoms (Si I) and singly (Si II and C II) and doubly (Si III) charged ions [29]. It is interesting to note the presence of highly charged ions at this short delay. Measurements (not shown) with a time-delayed acquisition gate by a time as short as 50 ns do not contain these emissions,

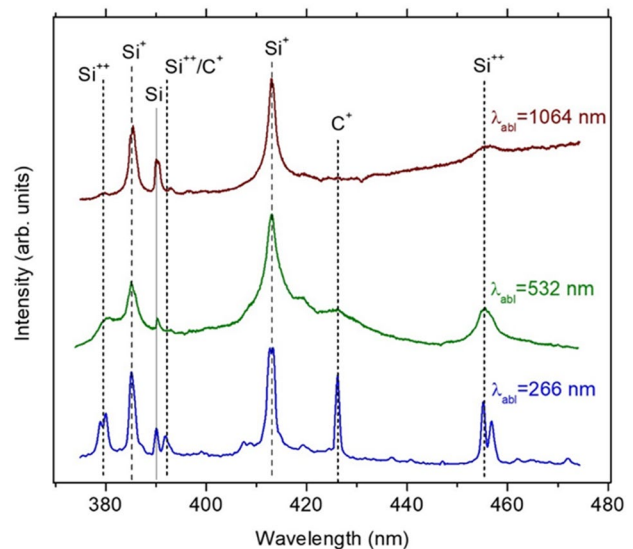


Fig. 1 Optical emission spectra acquired during ablation of SiC at 1064, 532 and 266 nm in the spectral region of 375–475 nm. Spectra were collected in a time window of 100 ns after the ablation event. Spontaneous emissions from C^+ , Si, Si^+ and Si^{++} are detected in this region

an indication of very fast recombination dynamics in the plasma.

Analysis of the OES spectra yields further information on the characteristics of the plasma and its variations with changes in the laser ablation wavelength. Even though all the cases presented are moderately ionized plasmas, some differences are clear. Most notably, the presence of highly ionized species, such as Si^{++} and C^+ , with respect to lower charge species, such as Si or Si^+ , is favored for the shorter laser wavelength employed, i.e., 266 nm. Thus, the distribution of charged species in the plasma seems to be shifted towards higher values of the charge for UV wavelengths with respect to visible/IR wavelengths. This higher ionization for shorter laser wavelengths has been observed before [28, 30, 31] and can be attributed to the much higher absorption coefficient of SiC at 266 nm than in the visible-IR [32], causing stronger laser-target coupling and thus higher excitation in the plasma. The consequences of these different plasmas on the characteristics of the deposited SiC films will be discussed below.

3.2 Physicochemical characterization of the laser-deposited thin films

AFM characterization of some of the SiC deposited films—those grown on STO (100)—for low and high temperature (300 K and 1025 K) are shown in Fig. 2. AFM images of deposits on Si (100) present no substantial differences. The thickness of the films was evaluated through the use

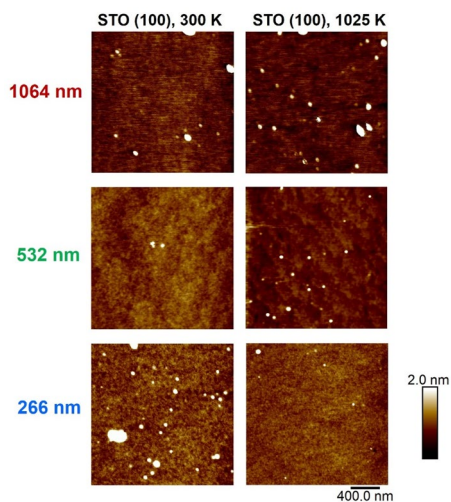


Fig. 2 Height AFM images of SiC deposits obtained on STO (100) at the laser wavelengths and substrate temperatures indicated on the figure

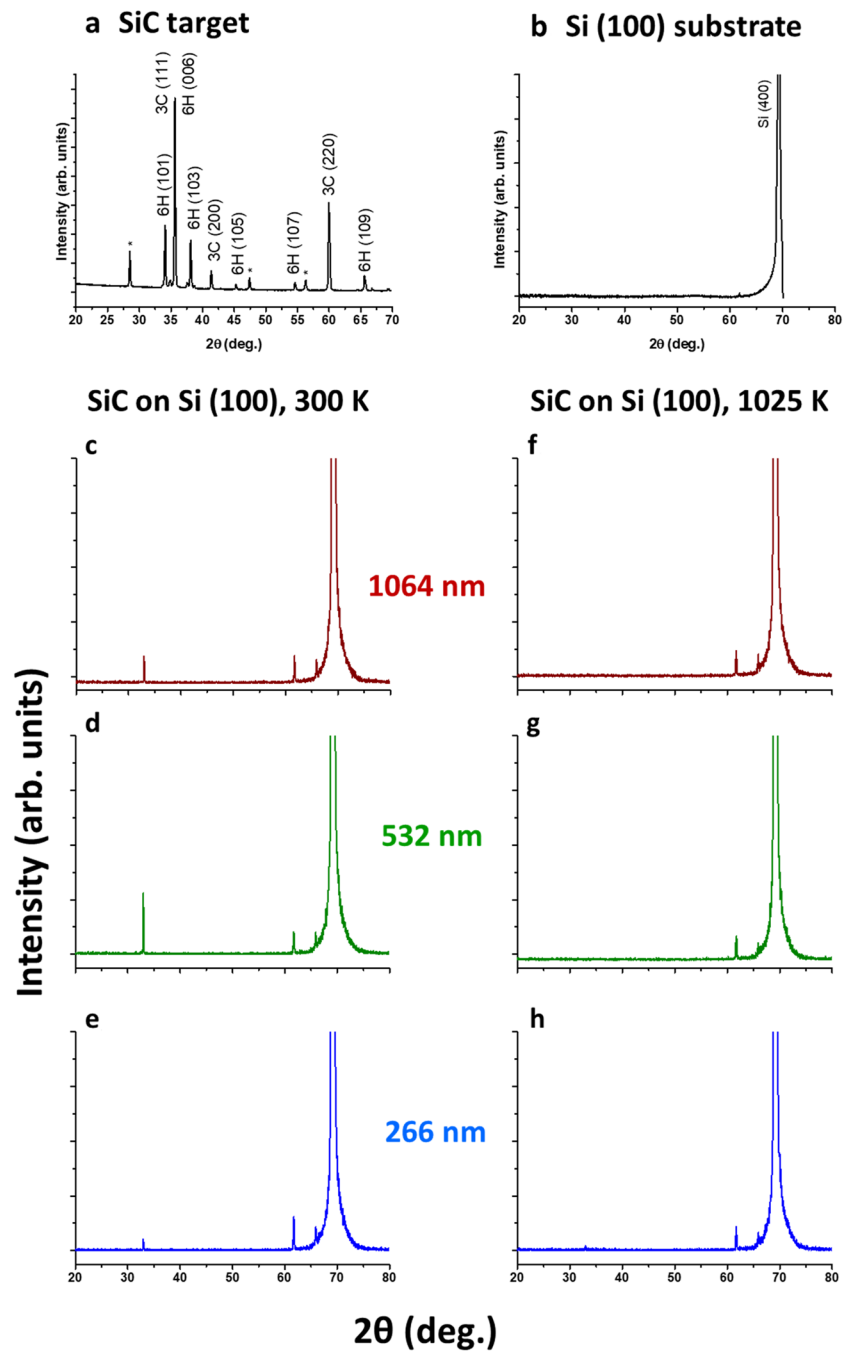
of a mask that partially covered the substrates; values in the range of 30–100 nm were found, which corresponds to deposition rates of the order of 0.01 nm/s. This deposition rate is comparable to some other PLD works [21] but an order of magnitude lower than the deposition rate obtained for instance in refs. [11] or [7] with the hot-wire chemical vapor deposition method. In relation to the effect of laser wavelength and temperature, no clear trends were detected as a function of wavelength, which is likely to be a consequence of the different fluence employed at each wavelength to be sufficiently above the ablation threshold. Contrarily, we systematically observe a lower deposition rate for higher temperature, which is consistent with the deposition of a denser, more highly ordered structure. Notably, it is observed that, in all cases, the root mean square roughness measured in $10\ \mu\text{m} \times 10\ \mu\text{m}$ AFM topography images (see Fig. S1) is below 3 nm, with an average value over all deposits as low as 1.7 ± 0.7 nm. Very low roughness values found in SiC laser deposited films had been reported previously [18], where films fabricated at temperatures between 750 and 1050 K were extremely smooth with average roughness of the order of 0.4 ± 0.2 nm (measured in $1\ \mu\text{m} \times 1\ \mu\text{m}$ AFM images), in agreement with the values obtained in this work (average roughness of all the deposits in this work in $10\ \mu\text{m} \times 10\ \mu\text{m}$ areas is 0.6 ± 0.3 nm). Interestingly, in reference [18], the roughness was found to increase substantially above a temperature threshold of around 1100 K, with a roughness of 4.7 ± 0.8 nm for the film deposited at 1220 K. This qualitative change in the surface quality of the deposits was attributed to the formation of large crystallites, i.e., the temperature onset for crystallization. Since our work was performed at temperatures below this onset, the roughness

values found are very low across our study, with surfaces of extremely good quality.

Regarding the evaluation of film structure, Fig. 3 displays Cu-K α -based XRD features of thin films deposited on Si (100) substrates. As a reference, in the top part of Fig. 3, the XRD patterns of the original SiC target (with 3C and 6H components) and of the bare Si substrate are shown. Four peaks can be appreciated in the XRD results, but they all correspond to crystalline silicon (lattice parameter $a = 0.357$ nm). Due to the extinction rules, only the (400) reflection should be allowed, and this corresponds to the strongest peak seen at 69.16° . We can also see the forbidden (200) reflection at 32.97° due to second-order diffraction. The other minor peaks detected at 61.68° and 65.87° all correspond to Si (400) but caused by contamination of the source, i.e., they do not correspond to diffraction of the Cu K α radiation, but to Cu K β and W L α radiation, respectively. Similarly, results obtained from deposits on STO (100) (not shown) only reveal peaks corresponding to the substrate and not to the deposit. The absence of peaks assignable to SiC structures cannot be attributable to the thin nature of the films, since the thicknesses measured by AFM are sufficient for XRD measurements. Therefore, the results indicate that the deposited films are overall amorphous. This is in good agreement with previous literature on this material, for which several authors [33–35] have reported that crystalline films only appear for T_s above 1075 K.

Raman measurements of the silicon carbide target as well as of thin films grown on Si (100) and STO (100) substrates were obtained. As illustration, Fig. 4 shows the Raman spectra corresponding to the SiC bulk and grown thin films upon 532 nm laser irradiation on the Si (100) substrate at low (300 K) and high (1025 K) temperature. For bulk SiC (black curve in Fig. 4), five characteristic Raman peaks can be detected by close inspection. Those with 796 and 972 cm^{-1} Raman shifts were assigned to the cubic polytype structure 3C-SiC; the peak at 796 cm^{-1} corresponding to the transverse optical (TO) phonon mode, and that at 972 cm^{-1} , to the longitudinal optical (LO) phonon mode. The hexagonal modes for 6H-SiC are revealed by the additional TO modes at 767 cm^{-1} and 789 cm^{-1} , and the LO mode at 965 cm^{-1} . This is in agreement with previously published data [36] and is a result of the polycrystalline nature of the SiC targets. In addition to the SiC Raman peaks, other Raman contributions were observed at 297, 470, 521, 620 and 938–987 cm^{-1} , which were assigned to the crystalline silicon substrate. For room temperature PLD deposits (solid blue line in Fig. 4), Raman peaks are attributed to the silicon substrate, with no evidence for those corresponding to SiC. At these conditions, an additional minor peak is detected at 433 cm^{-1} , which could be assigned to network bending modes of an oxidized layer of SiO $_2$ [37]. For the films deposited at 1025 K, in addition to the silicon substrate peaks, a

Fig. 3 X-ray diffraction data. The box at the top shows the X-ray diffractogram of the original SiC target (a) and the bare Si(100) substrate (b). The rest of the plots show X-ray diffractograms from SiC thin films grown by PLD at 1064 (c, f), 532 (d, g) and 266 nm (e, h) on Si (100) substrates at 300 K (left column) and 1025 K (right column). The peaks indicated with an asterisk in panel (a) are tentatively assigned to SiO₂



weak broad band is observed with a Raman shift centered at 820 cm^{-1} , which can be assigned to the presence of amorphous silicon carbide [20, 38]. In this case, a second, intense broad band is also observed in the range of $1200\text{--}1700\text{ cm}^{-1}$, which is characteristic of amorphous carbon with a disordered network of C–C bonds [39]. The presence of these bands is common to all films deposited at high temperature. These results indicate that higher temperatures during the deposition process favor the growth of disordered carbon and SiC (the carbon bands were also observed for deposits grown at high temperature on STO). Raman characterization

was also performed on SiC deposits at wavelengths of 1064 and 266 nm on both substrates. The results (not shown) were analogous to those obtained at 532 nm on Si (100). The lack of clear Raman peaks corresponding to SiC bonds in the deposits is related to the non-crystalline nature of these films, but important changes are evident as a function of temperature, with the emergence of a band attributable to Si–C bonds together with disordered carbon at 1025 K.

Information on the atomic composition and chemical state of the surface layer of the targets and the synthesized materials was obtained by XPS. The XPS Si $2p$ spectrum

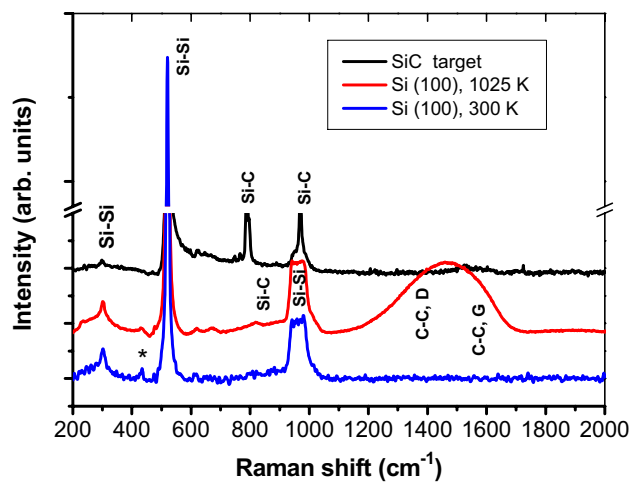


Fig. 4 Micro-Raman measurements of the SiC target (solid black line) and PLD thin films grown at 532 nm on Si (100) substrates at 300 K (solid blue line) and 1025 K (solid red line). An asterisk marks a peak tentatively assigned to an oxidized layer of SiO₂

recorded from the SiC target, shown in Fig. 5a, contains two clearly different spin orbit doublets, one characterized by a binding energy (BE) of the Si 2p_{3/2} core level at 101.0 eV, which is characteristic of SiC, and a second, minor one located at a BE of the Si 2p_{3/2} of 102.4 eV, which can be associated to SiO₂. The respective spectral areas of the SiC and SiO₂ contributions obtained from the fit of the spectrum are 70% and 30%, respectively. The C 1s core level spectrum (not shown) consists of four components: one located at 282.5 eV, due to bulk SiC, and three additional peaks at 285.0, 286.4, 288.7 ± 0.1 eV due to C–C, C–O–C and O–C=O bonds, respectively. The latter are the typical constituents of the adventitious carbon contamination layer. These measurements clearly indicate the presence of an (expected) oxidized layer on the original targets.

The high-resolution Si 2p XPS spectra recorded for the different laser deposited thin films on STO (100) are shown in Fig. 5b–g. They were best fitted, in all cases, to two different contributions with binding energies characteristic of SiC (blue component, with lower binding energies) and SiO₂ (green component, with higher binding energies, see above). The relative areas of the two contributions obtained from the fitted spectra are collected in Table 1. Inspection of Fig. 5b–g and Table 1 shows the dramatic change of surface composition with T_S, with a predominant SiC component of the XPS signals only appearing for deposition at high temperature (1025 K). It must be noted that the typical penetration depth of XPS analyses is ≤ 4 nm, due to the short mean free path of the generated photoelectrons, and thus the XPS analysis can only reveal the surface composition of the films. In any case, the results show that the surface layer of the deposits is dominated by SiO₂ if PLD is carried out

at room temperature, whereas it is mainly composed of SiC for 1025 K. It is important to recall that Raman measurements (Fig. 4), which are sensitive to thicknesses up to a few microns, and thus to the full depth of the deposited films, do not show any bands attributable to Si–O bonds. Therefore, the combined XPS and Raman results indicate that the presence of SiO₂ is only superficial in the films. This is consistent with the findings of Katharria et al. in their paper on UV PLD of SiC [20], where they reported the formation of Si–O bonding in PLD films through XPS. To investigate this effect, they performed XPS measurements after different doses of Ar ion sputtering of the films. Their results clearly reveal that as the sputtering dose increases—i.e., analysis of deeper layers of the film is made possible—the proportion of oxygen bonds rapidly decreases.

Our finding that the oxygen content of the deposited films decreases at higher T_S is consistent with previous reports [21, 22]. Of particular relevance to this matter is the SiC PLD work by P.P. Dey et al. [6], where FTIR measurements showed that as T_S was risen from 300 K to 1025 the intensity of the absorption coefficient of the vibrational modes related to the presence of oxygen gradually decreased, until for the highest temperature of 1025 K the films were practically oxygen free.

The XPS data displayed here effectively show that the (low) proportion of SiO₂ for the higher T_S employed (1025 K) is roughly independent of the laser wavelength, with superficial SiC concentration in values of ≈ 80%. Contrarily, it is interesting to note that, for the deposits grown at room temperature, significant variations of superficial SiO₂ are found, as the XPS signal is entirely dominated by SiO₂ for IR PLD and an increasing proportion of SiC emerges as the PLD wavelength is shortened through the visible and into the ultraviolet. Thus, short wavelength PLD tends to mimic the desirable behavior of high-temperature substrates in this respect.

In summary, our work shows that the morphology, as measured by AFM, and crystallinity, as measured by XRD, of the pulsed laser-deposited SiC films are extremely robust against changes either in the T_S, in the 300–1025 K range, or in the ablation wavelength, i.e., extremely smooth amorphous SiC films are grown under all conditions. Comparison with previous literature allows us to estimate that the highest temperature used in our study, 1025 K, is situated right below the onset of the observation of crystallinity. In Ref. [6] this can be appropriately visualized in images obtained with FESEM (Field effect Scanning Electron Microscopy) in combination with SAED (Selected Area Electron Diffraction). These studies show the gradual appearance of particulates in the films as temperature rises from 300 to 1025 K, and demonstrate that at 1025 K, even though the film remains globally amorphous, it does contain nanocrystalline domains. Our Raman data

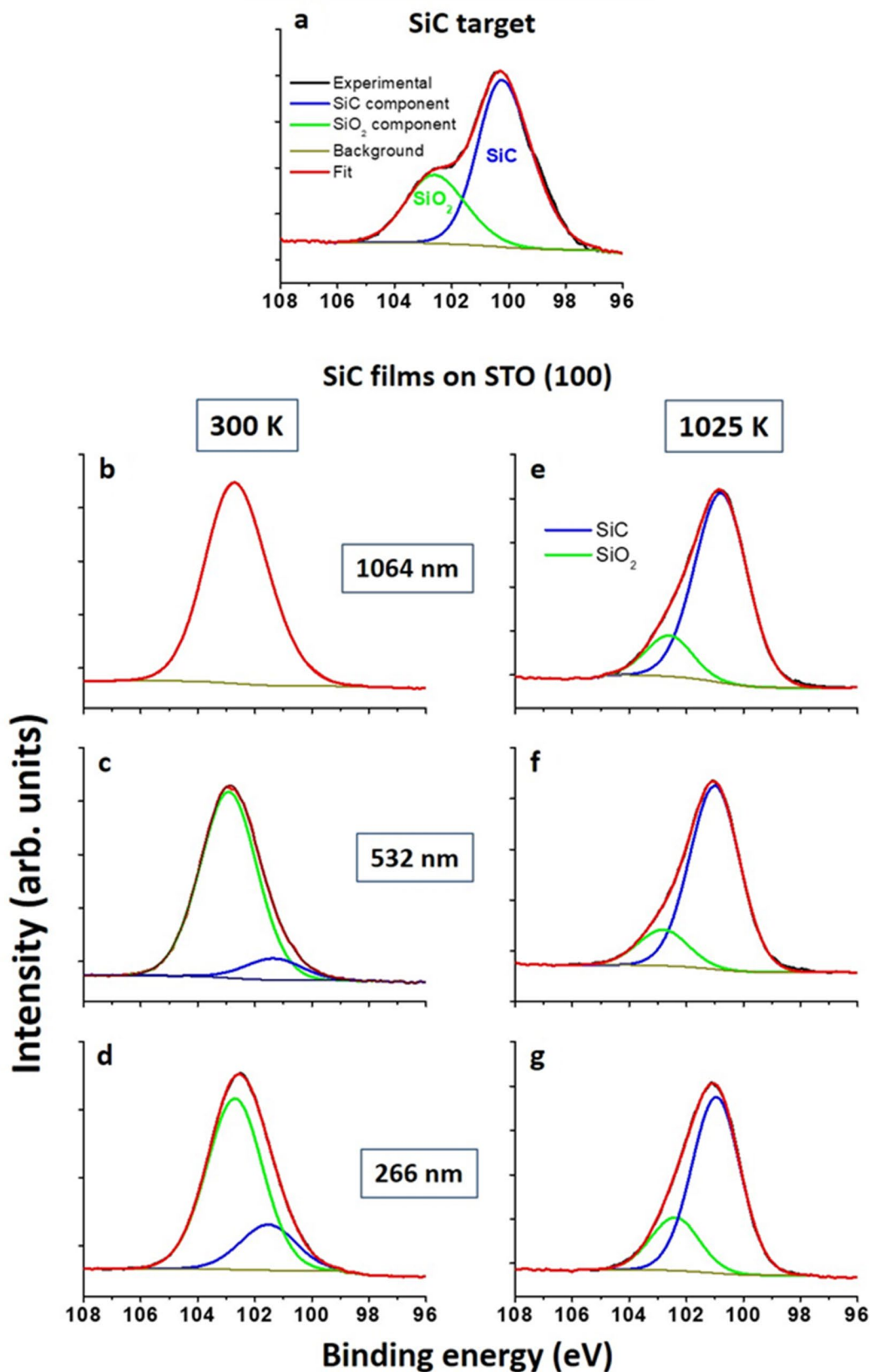


Fig. 5 XPS Si 2p core level spectra recorded from the SiC target (a) and the PLD thin films grown at 1064 (b, e), 532 (c, f) and 266 nm (d, g) on STO (100) substrates at 300 K (left column) and 1025 K (right column)

Table 1 SiC and SiO₂ ratios (in %) as determined by XPS measurements on deposited thin films upon laser irradiation at 1064, 532 and 266 nm on STO (100) substrates at 300 K and 1025 K

Wavelength (nm)	300 K		1025 K	
	SiC	SiO ₂	SiC	SiO ₂
1064	0	100	84	16
532	10	90	84	16
266	21	79	77	23

The values are affected by errors of the order of 5%

offer a hint of this densification that is the prelude to crystallinity through the appearance of the weak Si–C band at 820 cm⁻¹ for 1025 K PLD.

This relatively robust behavior of the properties of the films as a function of laser ablation wavelength contrasts with previous PLD observations with other semiconductor materials [40–42], where clear differences were found regarding thickness, nanostructure and crystallinity of deposits, and in this sense, our results for this material show that production of amorphous, extremely smooth SiC thin films is possible with any laser source producing nanosecond pulses with sufficient intensity across the spectrum from the UV to the IR.

The clearest differences measurable for the different growth conditions have been observed through the XPS measurements. With respect to temperature, higher T_S favors the mobility of atoms arriving into the surface, enabling them to find thermodynamically favorable sites. A higher number of Si–C bonds are formed in these conditions, which promotes the growth of a compact structure that can make these SiC films appropriate for applications like protective coatings. Contrarily, at lower T_S , the surface atom mobility is severely limited, leading to the formation of dangling bonds, which favors the formation of a strongly oxidized layer on the film upon exposure to air. An additional factor favoring the lower fraction of SiO₂ for higher deposition temperatures is the possible contribution of O₂ evaporation.

Our results show that, for high T_S , atom mobility is dominated by temperature, with a residual role of the laser wavelength. However, it is interesting to note that for low T_S —room temperature growth—, we observe that shorter wavelengths tend to mimic the high T_S behavior. As was described in the first part of this section, the ablation plasmas obtained with UV ablation showed increased excitation in the form of species with higher ionic charges than those observed for the longer ablation wavelengths. This will necessarily lead to higher particle kinetic energies, which can cause thermal transients in the target surface upon arrival, sufficient to enhance atom mobility and thus enhance the

formation of a higher number of Si–C bonds. This result shows that in cases when it is not feasible to increase T_S , finding the laser source that maximizes the kinetic energies of the plasma particles is an alternative route to synthesize SiC films of higher density and thus better quality.

4 Conclusions

The capabilities of controlling the physicochemical properties of thin films deposited on different substrates upon ablation of silicon carbide targets with different laser wavelengths and environmental conditions have been explored. To that purpose, films of silicon carbide were obtained by pulsed laser deposition on Si (100) and STO (100) substrates at room temperature (300 K) and at 1025 K upon ablation using a Nd:YAG laser emitting at 1064, 532 and 266 nm.

Atomic force microscopy indicates that the deposits are extremely smooth, although in some cases, the presence of some particulates is appreciated. Micro-Raman spectroscopy and X-ray diffraction indicate that the deposited silicon carbide films were amorphous under all the experimental conditions used. In turn, X-ray photoelectron spectroscopy indicates that the composition of the superficial layer of the deposited films is a mixture of silicon dioxide and silicon carbide. The contribution of the latter is crucially favored by the increase in substrate temperature to 1025 K. For lower PLD temperatures (room temperature), this contribution can also be higher at lower ablation wavelengths.

Supplementary Information The online version contains supplementary material available at <https://doi.org/10.1007/s00339-022-05499-9>.

Acknowledgements This research was supported by the Spanish State Research Agency (AEI) and European Regional Development (FEDER) through Projects PID2019-106125GB-I00/AEI/0.13039/501100011033 and PID2019-104124RB-I00/AEI/0.13039/501100011033. Thanks are given to the Soft and Polymeric Matter group (IEM-CSIC) for the use of AFM. We are grateful to M. Furió from MNCN-CSIC and P. Gonzalez from ICTP-CSIC for Raman and X-ray diffraction technical assistance, respectively.

Funding Open Access funding provided thanks to the CRUE-CSIC agreement with Springer Nature.

Open Access This article is licensed under a Creative Commons Attribution 4.0 International License, which permits use, sharing, adaptation, distribution and reproduction in any medium or format, as long as you give appropriate credit to the original author(s) and the source, provide a link to the Creative Commons licence, and indicate if changes were made. The images or other third party material in this article are included in the article's Creative Commons licence, unless indicated otherwise in a credit line to the material. If material is not included in the article's Creative Commons licence and your intended use is not permitted by statutory regulation or exceeds the permitted use, you will

need to obtain permission directly from the copyright holder. To view a copy of this licence, visit <http://creativecommons.org/licenses/by/4.0/>.

References

- N.G. Wright, A.B. Horsfall, K. Vassilevski, Prospects for SiC electronics and sensors. *Mater. Today* **11**, 16–21 (2008)
- H.O. Pierson, *Handbook of Refractory Carbides and Nitrides: Properties, Characteristics, Processing and Applications* (William Andrew, 1996)
- J. Fan, P.K. Chu, Group IV nanoparticles: synthesis, properties, and biological applications. *Small* **6**, 2080–2098 (2010)
- J. Fan, P.K. Chu, *Silicon Carbide Nanostructures: Fabrication, Structure, and Properties* (Springer, 2014)
- M.A.E. Khakani, M. Chaker, M.E. O'Hern, W.C. Oliver, Linear dependence of both the hardness and the elastic modulus of pulsed laser deposited a-SiC films upon their Si–C bond density. *J. Appl. Phys.* **82**, 4310–4318 (1997)
- P.P. Dey, A. Khare, Effect of substrate temperature on structural and linear and nonlinear optical properties of nanostructured PLD a-SiC thin films. *Mater. Res. Bull.* **84**, 105–117 (2016)
- F. Shariatmadar Tehrani, B.T. Goh, M.R. Muhamad, S.A. Rahman, Pressure dependent structural and optical properties of silicon carbide thin films deposited by hot wire chemical vapor deposition from pure silane and methane gases. *J. Mater. Sci. Mater. Electron.* **24**, 1361–1368 (2013)
- A.K. Costa, S.S. Camargo, Amorphous SiC coatings for WC cutting tools. *Surf. Coat. Technol.* **163**, 176–180 (2003)
- H. Matsunami, S. Nishino, H. Ono, IVA-8 heteroepitaxial growth of cubic silicon carbide on foreign substrates. *IEEE Trans. Electron Devices* **28**, 1235–1236 (1981)
- D.C. Lim, H.G. Jee, J.W. Kim, J.S. Moon, S.B. Lee, S.S. Choi, J.H. Boo, Deposition of epitaxial silicon carbide films using high vacuum MOCVD method for MEMS applications. *Thin Solid Films* **459**, 7–12 (2004)
- A. Tabata, Y. Komura, T. Narita, A. Kondo, Growth of silicon carbide thin films by hot-wire chemical vapor deposition from SiH₄/CH₄/H₂. *Thin Solid Films* **517**, 3516–3519 (2009)
- U. Coscia, G. Ambrosone, C. Minarini, V. Parisi, S. Schutzmann, A. Tebano, Structural modification of laser annealed a-Si_{1-x}C_x: H films. *Appl. Surf. Sci.* **252**, 4493–4496 (2006)
- X.T. Zhou, N. Wang, H.L. Lai, H.Y. Peng, I. Bello, N.B. Wong, C.S. Lee, S.T. Lee, β -SiC nanorods synthesized by hot filament chemical vapor deposition. *Appl. Phys. Lett.* **74**, 3942–3944 (1999)
- R. Eason, *Pulsed Laser Deposition of Thin Films: Applications-Led Growth of Functional Materials* (Wiley, Berlin, 2007)
- D.B. Chrisey, G.K. Hubler, *Pulsed laser deposition of thin films* (John Wiley and sons inc, Newyork, 1994)
- T. Kusumori, H. Muto, M.E. Brito, Control of polytype formation in silicon carbide heteroepitaxial films by pulsed-laser deposition. *Appl. Phys. Lett.* **84**, 1272–1274 (2004)
- B. Pecholt, S. Gupta, P. Molian, Review of laser microscale processing of silicon carbide. *J. Laser Appl.* **23**, 012008 (2011)
- M. Tabbal, A. Said, E. Hannoun, T. Christidis, Amorphous to crystalline phase transition in pulsed laser deposited silicon carbide. *Appl. Surf. Sci.* **253**, 7050–7059 (2007)
- I. Hanyecz, J. Budai, A. Oszkó, E. Szilágyi, Z. Tóth, Room temperature pulsed laser deposition of Si₆C thin films in different compositions. *Appl. Phys. A* **100**, 1115–1121 (2010)
- Y.S. Katharria, S. Kumar, R.J. Choudhary, R. Prakash, F. Singh, N.P. Lalla, D.M. Phase, D. Kanjilal, Pulsed laser deposition of SiC thin films at medium substrate temperatures. *Thin Solid Films* **516**, 6083–6087 (2008)
- V. Craciun, E. Lambers, N.D. Bassim, R.H. Baney, R.K. Singh, Growth of dense SiC films on Si at medium temperatures by pulsed laser deposition. *J. Vac. Sci. Technol., A* **19**, 2691–2694 (2001)
- G. Socol, A.C. Galca, D. Craciun, M. Hanna, C.R. Taylor, E. Lambers, V. Craciun, Pulsed laser deposition of nanocrystalline SiC films. *Appl. Surf. Sci.* **306**, 66–69 (2014)
- M. Filipescu, G. Velisa, V. Ion, A. Andrei, N. Scintee, P. Ionescu, S.G. Stanciu, D. Pantelica, M. Dinescu, Silicon carbide thin films as nuclear ceramics grown by laser ablation. *J. Nucl. Mater.* **416**, 18–21 (2011)
- Y.H. Tang, T.K. Sham, D. Yang, L. Xue, Preparation and characterization of pulsed laser deposition (PLD) SiC films. *Appl. Surf. Sci.* **252**, 3386–3389 (2006)
- H. ElGazzar, E. Abdel-Rahman, H.G. Salem, F. Nassar, Preparation and characterizations of amorphous nanostructured SiC thin films by low energy pulsed laser deposition. *Appl. Surf. Sci.* **256**, 2056–2060 (2010)
- A. Keffous, K. Bourenane, M. Kechouane, N. Gabouze, T. Kerdja, Morphological, structural and optical properties of thin SiC layer growth onto silicon by pulsed laser deposition. *Vacuum* **81**, 632–635 (2007)
- G. Monaco, D. Garoli, M. Natali, M.G. Pelizzo, P. Nicolosi, Synthesis of heteroepitaxial 3C-SiC by means of PLD. *Appl. Phys. A* **105**, 225–231 (2011)
- M. Oujja, L. Martín-García, E. Rebolgar, A. Quesada, M.A. García, J.F. Fernández, J.F. Marco, J. de la Figuera, M. Castillejo, Effect of wavelength, deposition temperature and substrate type on cobalt ferrite thin films grown by pulsed laser deposition. *Appl. Surf. Sci.* **452**, 19–31 (2018)
- A. Kramida, Y. Ralchenko, J. Reader, NIST Atomic Spectra Database (version 5.6. 1) (2018), URL <https://physics.nist.gov/asd>. National Institute of Standards and Technology, Gaithersburg, MD (2018). Accessed 1 Oct 2021
- A.E. Hussein, P.K. Diwakar, S.S. Harilal, A. Hassanein, The role of laser wavelength on plasma generation and expansion of ablation plumes in air. *J. Appl. Phys.* **113**, 143305 (2013)
- L. Torrisi, S. Gammino, L. Andò, V. Nassisi, D. Doria, A. Pedone, Comparison of nanosecond laser ablation at 1064 and 308 nm wavelength. *Appl. Surf. Sci.* **210**, 262–273 (2003)
- G. Derst, C. Wilbertz, K.L. Bhatia, W. Kratschmer, S. Kalbitzer, Optical properties of SiC for crystalline-amorphous pattern fabrication. *Appl. Phys. Lett.* **54**, 1722–1724 (1989)
- L. Rimai, R. Ager, J. Hangas, E.M. Logothetis, N. Abu-Ageel, M. Aslam, Pulsed laser deposition of SiC films on fused silica and sapphire substrates. *J. Appl. Phys.* **73**, 8242–8249 (1993)
- T. Zehnder, A. Blatter, A. Bächli, SiC films prepared by pulsed excimer laser deposition. *Thin Solid Films* **241**, 138–141 (1994)
- J.S. Pelt, M.E. Ramsey, S.M. Durbin, Characterization of crystalline SiC films grown by pulsed laser deposition. *Thin Solid Films* **371**, 72–79 (2000)
- S. Nakashima, H. Harima, Raman investigation of SiC polytypes. *Phys. Status Solidi A* **162**, 39–64 (1997)
- E.L. Lee, I.E. Wachs, In situ raman spectroscopy of SiO₂-supported transition metal oxide catalysts: an isotopic ¹⁸O–¹⁶O exchange study. *J. Phys. Chem. C* **112**, 6487–6498 (2008)
- G. Leal, T.M.B. Campos, A.S.D. Sobrinho, R.S. Pessoa, H.S. Maciel, M. Massi, Characterization of SiC thin films deposited by HiPIMS, Materials research—Ibero-American. *J. Mater.* **17**, 472–476 (2014)

39. A.C. Ferrari, J. Robertson, Interpretation of Raman spectra of disordered and amorphous carbon. *Phys. Rev. B* **61**, 14095–14107 (2000)
40. I. Lopez-Quintas, M. Oujja, M. Sanz, A. Benitez-Cañete, R.J. Chater, M.V. Cañamares, J.F. Marco, M. Castillejo, Micrometric rods grown by nanosecond pulsed laser deposition of boron carbide. *Appl. Surf. Sci.* **328**, 170–176 (2015)
41. M. Sanz, M. López-Arias, J.F. Marco, R. de Nalda, S. Amoruso, G. Ausanio, S. Lettieri, R. Bruzzese, X. Wang, M. Castillejo, Ultrafast laser ablation and deposition of wide band gap semiconductors. *J. Phys. Chem. C* **115**, 3203–3211 (2011)
42. M. Sanz, M. López-Arias, E. Rebollar, R. de Nalda, M. Castillejo, Laser ablation and deposition of wide bandgap semiconductors: plasma and nanostructure of deposits diagnosis. *J. Nanopart. Res.* **13**, 6621–6631 (2011)

Publisher's Note Springer Nature remains neutral with regard to jurisdictional claims in published maps and institutional affiliations.